— 9 —

In-flight Comparisons of Solar EUV Irradiance Measurements Provided by the CELIAS/SEM on SOHO

DONALD R. MCMULLIN, DARRELL L. JUDGE
University of Southern California, Space Sciences Center
Los Angeles, California, USA

MARTIN HILCHENBACH
Max-Planck-Institut für Aeronomie
Katlenburg-Lindau, Germany

FRED IPAVICH
Department of Physics and Astronomy and IPST
University of Maryland, College Park, MD, USA

PETER BOCHSLER, PETER WURZ, ALFRED BÜRGI
Physikalisches Institut der Universität Bern
Bern, Switzerland

WILLIAM T. THOMPSON
L3 Communications Analytics Corporation
NASA GSFC, Greenbelt, MD, USA

JEFFREY S. NEWMARK
Naval Research Laboratory
Washington, DC, USA

Since 1 January 1996, the Solar EUV Monitor (SEM) on the Solar and Heliospheric Observatory (SOHO) has continuously measured the solar EUV irradiance. The SEM monitors the full-disk irradiance from 0.1 nm to 50 nm in a broadband channel and also within an 8 nm wide bandpass centered at 30.4 nm. SEM irradiance measurements have been monitored periodically during the SOHO mission using sounding rockets. Through this in-flight calibration program, modest instrument degradation has been identified and corrected for in the published datasets. The relative standard uncertainty (1 σ) of SEM irradiance measurements is $\approx$ 10 %. The 81-d average of the calibrated SEM dataset shows an increase in EUV irradiance of a factor of three during the rise phase of solar cycle 23. The absolute value of the solar irradiance in the two SEM bands is also in agreement with measurements of the solar irradiance determined by ionization cells. The calibrated SEM irradiance values have been compared with irradiance values derived independently from SOHO/CDS and SOHO/EIT observations. The CDS and EIT irradiance values agree with the SEM within the combined uncertainties of the measurements.

9.1 Introduction

The Solar EUV Monitor (SEM) on the Solar and Heliospheric Observatory (SOHO) is integrated as part of the Charge, Element, and Isotope Analysis System (CELIAS). The CELIAS instrument on SOHO is designed to study the composition of the solar wind and of solar and interplanetary energetic particles [*Hovestadt et al.*, 1995]. One of the specific science objectives of CELIAS was to study the composition and dynamics of interplanetary pick-up ions, which originate from neutral particles (inflowing interstellar neutral atoms) that are ionized either through solar photons or by charge exchange with solar-wind ions. The production of pick-up ions through photoionization required measurement of the absolute photoionizing solar flux. The SEM was accordingly included to provide such data.

9.2 Instrument Description

The SEM is a simple transmission-grating spectrometer that makes use of state-of-the-art technology in the EUV wavelength region [*Hovestadt et al.*, 1995; *Judge et al.*, 1998]. Briefly, it is a lightweight (0.480 kg) instrument that consists of a high-density transmission grating (5000 bars / mm) and a free-standing aluminum filter positioned immediately behind the 2 mm $\times$ 10 mm entrance aperture. The aluminum film reduces the heat load on the grating and limits the wavelength range to the aluminum transmission region. The dispersed light is detected by three highly efficient, aluminum-coated, silicon photodiodes located 200 mm behind the grating at the zero-order and two first-order positions at 30.4 nm. The zero-order detector (channel 2) primarily measures the solar irradiance shortward of 50 nm. Due to the high sensitivity of silicon photodiodes and the relatively high transmission of aluminum at short wavelengths, the zero-order channel is quite sensitive to solar X-rays shortward of approximately 5 nm. The first-order detectors (channels 1 and 3) measure the irradiance within an 8 nm bandpass centered at the 30.4 nm solar He II resonance line emission, and are nominally insensitive to soft X-rays (see *Judge et al.* [1998]).

9.3 Cleanliness

Cleanliness of the optical components was a consideration in the design of the SEM housing. Potential degradation of the aluminum filter due to solar-wind particles is minimized by solar-wind deflector plates placed in front of the SEM entrance aperture. Material selection was considered to minimize the possible outgassing of organic material within the optics chamber. The SEM electronics reside below the optical bench, and are separated by the two-chamber design. The single electronics board is mounted below the optical housing. The optics chamber of the SEM is allowed to vent out separately through the entrance aperture at the front of the instrument. Conversely, the electronics chamber is vented out through a sintered, stainless steel, porous plug at the bottom of the instrument.

Table 9.1: Uncertainty Summary.

Item	Description	Uncertainty (%)
1	Calibration	5.0
2	Solar Spectral Distribution	9.0
3	Entrance Aperture	1.0
4	Statistical	0.5
Net Uncertainty		10.4

9.4 Pre-launch Calibration Standards Used and Calibration Methods

The SEM was calibrated at the Synchrotron Ultraviolet Radiation Facility (SURF II) [*Furst et al.*, 1995; *Canfield*, 1987] at the National Institute of Standards and Technology (NIST) in Gaithersburg, Maryland, USA. The individual components of the SEM (filter, gratings, and detectors) were first calibrated separately. Then the instrument as a whole was calibrated using both monochromatic radiation (on beamline 9) and undispersed synchrotron radiation (on beamline 2). The calibration constant of the current-to-frequency conversion electronics, the transmission of the grating (at 25.5 nm, 30.4 nm, and 33.5 nm), the quantum yield of the aluminum coated photodiodes (from 5 nm to 80 nm), and the transmission of the free-standing aluminum filter (from 5 nm to 80 nm) were measured independently. The zero-order quantum sensitivity has been extended shortward of the measured calibration (5 nm to 80.0 nm) to 0.1 nm by theoretical modeling. Each of the three detectors was modeled based on the physical parameters of the materials used in the detector design. Using the thickness and transmission properties of silicon, silicon dioxide, aluminum, and aluminum oxide between 0.1 nm and 50 nm [*Henke et al.*, 1993] the quantum efficiency was calculated as a function of wavelength. Modeling over the entire wavelength range for the end-to-end instrument in-flight configuration established the instrument responsivity at all wavelengths that were not directly calibrated.

9.5 Uncertainty Analysis

To convert the SEM count rates into absolute solar EUV flux, a convolution of the relative solar EUV spectral distribution and instrument efficiency is necessary. In order to determine the absolute solar flux it is necessary to adopt a nominal solar EUV spectrum in order to weight the wavelength-dependent instrument quantum efficiencies, Q_λ (counts/photon), of the SEM spectrometer. In the present analysis, we have used the SOLERS22 composite spectral distribution [*Woods et al.*, 1998] divided into 1 nm bins. In addition to knowledge of the instrument response as a function of wavelength (λ) and the relative spectral distribution (β_λ), the accuracy of SEM irradiance values is also dependent on the uncertainty in the measurement of the entrance aperture (A) and the statistical uncertainty of the measured instrument output (count rate). The absolute value of the pre-flight calibration flux is provided by NIST. The total uncertainty is made up of the independent uncertainties listed in Table 9.1, summed in quadrature, and yields a total SOHO/SEM relative standard uncertainty of ≈ 10 % (1σ).

The convolution of β_λ and Q_λ yields an irradiance conversion factor K, given below (Equation 9.1), that, when multiplied by the net count rate (CR), represents the measured absolute solar EUV irradiance in the wavelength band of interest, Φ_{total} (Equation 9.2).

$$\mathrm{K} = \frac{1}{A\Sigma\beta_\lambda Q_\lambda} \tag{9.1}$$

where

$$\Phi_{\text{total}} = \mathrm{CRK} \tag{9.2}$$

It should be noted and emphasized here that the resultant total solar flux value reported is dependent on the relative spectral distribution (β_λ) used to determine the absolute flux measured by both the SOHO/SEM and the rocket calibration SEM. As can be seen in the equations above, any changes in instrument responsivity observed by comparing the results from the rocket SEM with the SOHO/SEM can be attributed to changes in Q_λ on SOHO. In this calculation the solar spectral distribution must be considered. For the analysis of SEM data, we have chosen a fixed relative spectral distribution for consistency. Since it is widely known and available in the literature, we have completed the final analysis of the flight data using the SOLERS22 composite spectral distribution. Given the sensitivity of the SEM irradiance values to different reference spectra, we have assigned a 9 % relative standard uncertainty to our data (see also Table 9.1). However, to check the uncertainty of the absolute flux values reported using the method described above, the SOHO/SEM results have also been re-evaluated using spectra derived from both SOHO/CDS and SOHO/EIT observations, and the irradiance results for all three instruments have been compared. This second analysis has shown that when adjusting for the changes in the solar spectrum, as observed by CDS or EIT, the SEM results remain within the original instrument uncertainty of 10 %. Details of the SEM inter-comparisons using the CDS and EIT spectral distributions are described in *Thompson et al.* [2002].

After converting the observed count rates to solar irradiances measured at L_1 (the SOHO spacecraft location), the irradiances are normalized to a distance of 1 AU for comparison with other such normalized data.

9.6 In-flight Calibration

From the beginning, monitoring the in-flight stability of the instrument responsivity over time was an integral part of the SEM program. A calibration rocket payload that carries an identical SEM instrument provides a direct check of the absolute flux observed from the SOHO/SEM. The rocket SEM instrument is calibrated both before and after flight to monitor any responsivity changes, which may have occurred. The rocket SEM was calibrated using the NIST SURF II beamline 9. From just before the launch of SOHO in December 1995 until August 1999, six calibration series at NIST and three calibration rocket flights of the CELIAS/SEM spectrometer have been completed. Over this period of time, the responsivity of the rocket SEM has been verified as unchanged [*Judge et al.*, 1999].

9.7 Changes in Responsivity

Changes in responsivity on SOHO are determined by comparing the SOHO/SEM measurements with the calibrated rocket SEM, and are checked independently through simultaneous, absolute solar-flux measurements using ionization cells (see Section 9.9). From these measurement points, we derive a function that describes the change in responsivity for the SOHO/SEM for each channel. Based on the calibration rocket flight results [*Judge et al.*, 1999], a modest decrease in responsivity has been observed in all three SOHO/SEM channels. In direct comparison with the calibrated rocket flight instrument, the SOHO/SEM channels 1 and 3 (first-order position) both show the same amount of responsivity loss while channel 2 (central order) shows a smaller loss in responsivity, as expected, based on the degradation model discussed below. This model was developed to provide a method to adjust and correct the irradiance values between calibration rocket flights. The corrected dataset has since been used in extensive comparisons with CDS and EIT results. A detailed description of these comparisons can be found in *Thompson et al.* [2002].

9.8 Degradation Analysis

Analysis of the loss of responsivity observed in the SOHO/SEM channels indicates a common source for the observed degradation. That is, channel 1 and channel 3 both show the same amount of loss of responsivity, yet they are both independent channels, from the detectors through the electronics. However, all three channels share a common aluminum filter placed directly behind the entrance aperture. The observed differences in loss of responsivity have been modeled assuming carbon deposition on the aluminum filter as the cause of loss of responsivity. That is, hydrocarbon molecules that come into contact with the forward aluminum film are polymerized by EUV radiation and thus deposited onto the surface. Since the hydrogen absorption cross section is negligible, the deposition onto the filter can be modeled as a carbon film. Considering the transmission of carbon as a function of wavelength, the smaller loss in responsivity (measured as loss of signal) observed in the central image channel is consistent with the differences in efficiency between the central channel (channel 2) and first-order channels (channels 1 and 3) since the absorption cross-section of carbon is wavelength dependent. This difference is clearly seen when looking at the loss in signal between the first two calibration rocket flights. Over a period of 400 d, when compared with the observations from the rocket clone instrument, the SOHO/SEM reported a loss in signal of 15 % in both channel 1 and channel 3, and only a 5 percent loss in channel 2. This ratio of loss between the first-order and central-order channels is consistent with the addition of hydrocarbon deposition on the forward aluminum filter. In this case, the equivalent of 5 nm of carbon can explain the degradation of responsivity, using the transmission of carbon modeled as a function of wavelength [*Henke et al.*, 1993]. The smaller loss of signal observed in channel 2, the central image, is due to the relatively higher percentage of signal in channel 2 due to short wavelength photons, where the transmission of carbon is much less than the transmission at 30 nm (where channels 1 and 3 are most sensitive). In a similar manner, by including the results from the third calibration rocket flight, an exponential curve can be fit to the deposition rate of carbon on the forward aluminum film. The exponential curve is a logical assumption since it is be-

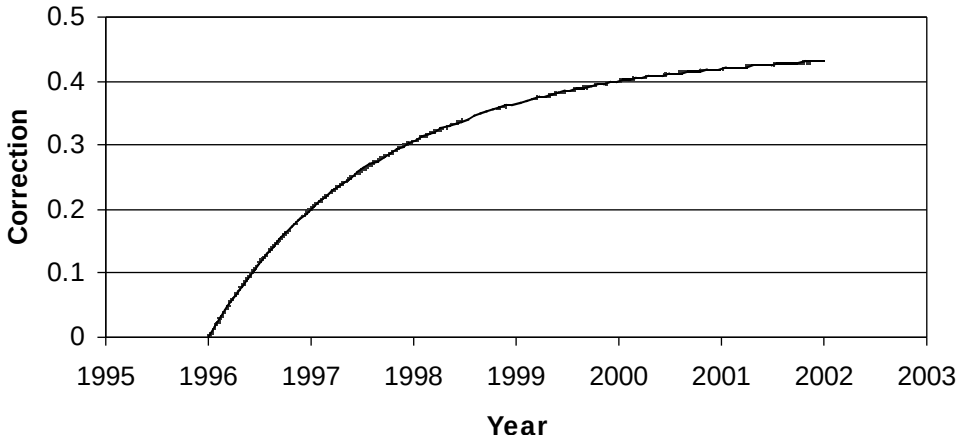

Figure 9.1: Correction to SEM results since 1 January 1996, based on sounding rocket calibration flight data.

lieved that the source of carbon contamination would be spacecraft outgassing. Using the initial pre-launch calibration as a starting point, and the subsequent three rocket flight data points to establish the carbon deposition rate, a simple model of loss of responsivity due to carbon deposition is used to correct the absolute value of the reported SEM irradiance. The time dependent correction derived from the three calibration points for the SEM is shown in Figure 9.1.

9.9 Comparisons

SEM irradiance values have been extensively compared with CDS and EIT irradiance results throughout the SOHO mission. A summary of these results can be found in *McMullin et al.* [2002a], with further details available in *Thompson et al.* [2002] and *Newmark et al.* [2002]. Briefly, the solar irradiance inter-comparisons of CDS and EIT to SEM, in the 26 nm to 34 nm band, are consistent within the instrument calibration uncertainties. These results are consistent when comparing the absolute value as well as the relative changes in solar irradiance over the solar cycle observed thus far (see Figure 9.2).

Additionally, the SEM results have been compared with simultaneous irradiance measurements provided by a Rare Gas Ionization Cell (RGIC) flown with the rocket calibration instrument. A detailed description of the ionization cell flown and the analysis method can be found in *Carlson* [1984]. A paper on the results from the ionization cell observations reported here is currently in preparation [*McMullin et al.*, 2002b]. The ionization cell flown for these measurements used neon gas, which provides the integral solar flux shortward of the ionization limit of neon. Correspondingly, the solar irradiance derived from the neon ionization cell is between $\approx$ 5 nm and 57.5 nm. The neon ionization cell yields measurements with an uncertainty of approximately 7 % [*Carlson*, 1984; *McMullin et al.*, 2002b]. This bandpass is very close to the SEM central-order bandpass of 0.1 nm to 50 nm. The results from the neon ionization cell are plotted with the SEM irradiance in Figure 9.3. The

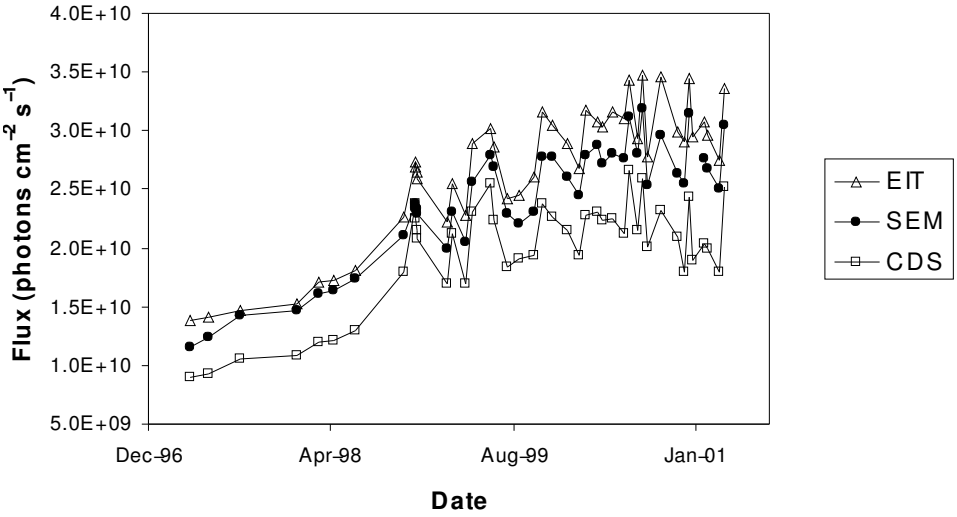

Figure 9.2: Absolute solar EUV irradiance from 26 nm to 34 nm from SEM, CDS, and EIT. All three measurements show similar trends in irradiance variability. Absolute values are within combined instrument calibration uncertainties.

inclusion of the neon absolute ionization detector in the calibration rocket payload provides independent in-flight verification of the absolute flux observed by the rocket SEM instrument in an overlapping wavelength range. As can be seen from the comparison, both instruments measured a similar increase in solar flux over the same time period, and agree within the respective measurement uncertainties. It is also interesting to note that for all three flights, the flux reported by the SEM 26 nm to 34 nm channel is approximately 50 % of the flux measured by the RGIC. These results indicate that the changes observed in the narrow band (26 nm to 34 nm) and the much wider band (5 nm to 57.5 nm) increase and decrease similarly, perhaps within a few percent, for a quasi-quiet Sun. That is, during the simultaneous measurements, there were no eruptive events producing a more than proportional increase of EUV flux in the short-wavelength band. This is also observed from the SEM central-order channel, which is very sensitive to changes in the soft X-ray flux during solar events [*Judge et al.*, 1998]. For quiet-Sun conditions, these two instruments have observed similar changes in the full-disk solar flux throughout the current solar cycle.

9.10 Helium Photoionization Rates

Using atomic cross-section data and the SEM-measured solar flux, the photoionization rate of helium is calculated. The ionization rate determined by this method using the SEM absolute flux is then compared against direct measurements as an independent verification of the absolute flux value reported. The SEM helium photoionization rates are determined by multiplying the measured wavelength dependent EUV irradiance by the helium pho-

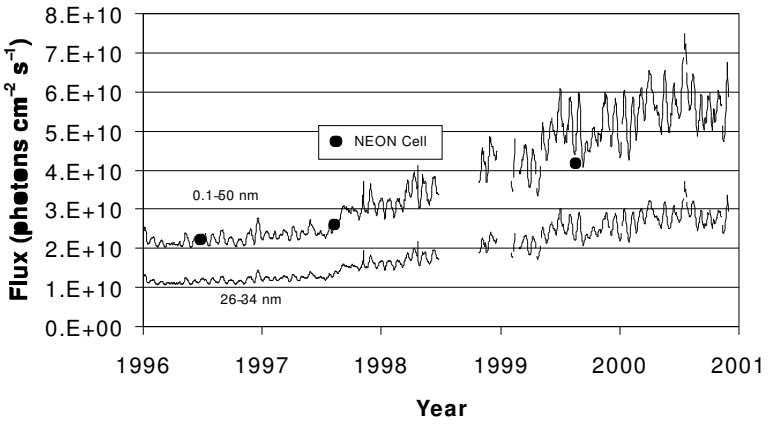

Figure 9.3: The absolute solar EUV irradiance at 1 AU from CELIAS/SEM 26 nm to 34 nm first-order and 0.1 nm to 50 nm central-order channels and the neon ionization cell flown at the same time.

toionization cross-section (in barn[1]) and then integrating the product over the ionizing wavelength range. The defining rate equation is

$$\nu = \int \Phi(\lambda)\sigma(\lambda)\mathrm{d}\lambda \tag{9.3}$$

In Equation (9.3), ν is the photoionization rate of helium in s^{-1}, $\Phi(\lambda)$ is the solar flux at wavelength λ in photons cm^{-2} s^{-1}, and $\sigma(\lambda)$ is the photoionization cross-section in barn, as a function of wavelength λ. This method has been used by *Banks and Kockarts* [1973], *Torr et al.* [1979] and *Torr and Torr* [1985]. The wavelength distribution of the integrated irradiance measured by the SEM is determined by using the relative solar spectrum given in *Woods et al.* [1998]. The absolute helium photoionization cross-section over the spectral region of interest is given by *Samson et al.* [1994]. The SEM-derived ionization results have been compared with direct measurements of the solar photoionization rate of helium by using a double-ionization helium gas cell [*Ogawa et al.*, 1997] to simultaneously measure the photoionization rate of helium. For these measurements, the helium ionization cell was flown on the Space Shuttle and simultaneous observations were coordinated with SOHO ICAL_12. The results of these measurements are described in detail by *McMullin et al.* [2002c]. This direct measurement of the helium ionization rate is in excellent agreement with the indirect results obtained by using the SEM flux data. Both results are shown in Figure 9.4.

9.11 Conclusions

The CELIAS/SEM on SOHO has provided the first continuous dataset of solar EUV irradiance measurements from solar minimum through solar maximum. The complete SEM dataset has shown good agreement with the limited full-disk observations available from

[1] 1 barn = 10^{-28} m^2

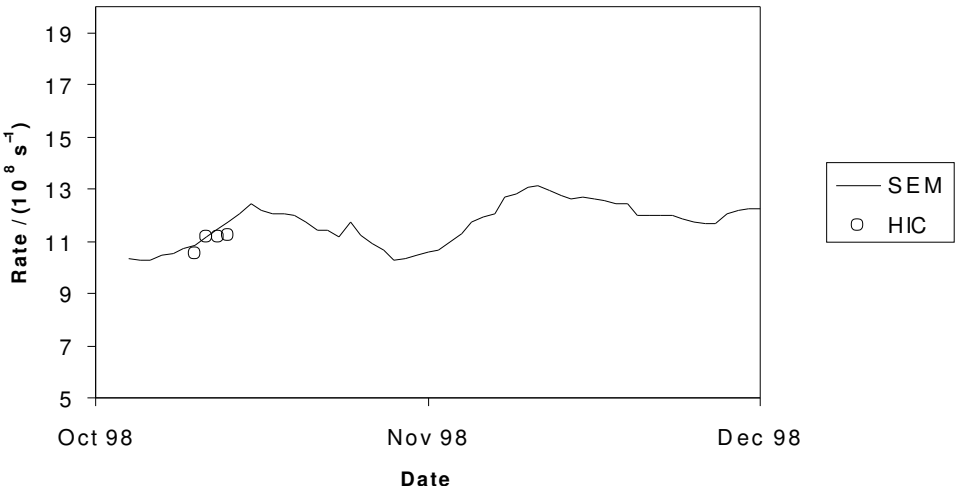

Figure 9.4: Helium photoionization rate derived from CELIAS/SEM irradiance data plotted with direct measurements for four days from the Helium Ionization Cell (HIC) flown on the Space Shuttle.

the SOHO CDS and EIT instruments in this same wavelength region in terms of the trend over the solar cycle, the variability throughout the cycle and the absolute value. On an absolute scale, the SEM irradiance values have been monitored throughout the SOHO mission by periodic rocket flights. These simultaneous rocket measurements have maintained the relative standard uncertainty of the SOHO/SEM dataset calibration at 10 %. Additionally, the absolute value is in good agreement with independent measurements from a rare-gas ionization cell flown simultaneously and with independent observations of the photoionization rate of helium.

Acknowledgements

This work has been supported by the National Aeronautics and Space Administration under grant No. NAG-5333 issued through the Office of Space Science, the Swiss National Science Foundation, and the PRODEX programme of ESA. Author JSN received support from NRL, the Office of Naval Research and NASA grant NDPRS-92385.

Bibliography

Banks, P.M., and Kockarts, G., Aeronomy, part A, Academic, San Diego, Calif., 1973.

Canfield, L.R., New far UV detector calibration facility at the National Bureau of Standards, *Appl. Opt.* **26**, 3831, 1987.

Carlson, R.W., Ogawa, H.S., Phillips, E., and Judge, D.L., Absolute measurement of the extreme UV solar flux, *Appl. Opt.* **23**, 2327–2332, 1984.

Furst, M.L., Graves, R.M., Canfield, L.R., and Vest, R.E., Radiometry at the NIST SURF II storage ring facility, *Rev. Sci. Instrum.* **66**, 2257, 1995.

Henke, B.L., Gullikson, E.M., and Davis, J.C., X-ray interactions: photoabsorption, scattering, transmission, and reflection at E=50–30000 eV, Z=1–92, *Atomic Data and Nuclear Data Tables* **54** (no. 2), 181, 1993.

Hovestadt, D., Hilchenbach, M., Bürgi, A., Klecker, B., Laeverenz, P., Scholer, M., Grünwaldt, H., Axford, W.I., Livi, S., Marsch, E., Wilken, B., Winterhoff, H.P., Ipavich, F.M., Bedini, P., Coplan, M.A., Galvin, A.B., Gloeckler, G., Bochsler, P., Balsiger, H., Fischer, J., Geiss, J., Kallenbach, R., Wurz, P., Reiche, K.U., Gliem, F., Judge, D.L., Ogawa, H.S., Hsieh, K.C., Möbius, E., Lee, M.A., Managadze, G.G., Verigin, M.I., and Neugebauer, M., CELIAS – Charge, element, and isotope analysis system for SOHO, *Sol. Phys.* **162**, 441–481, 1995.

Judge, D.L., McMullin, D.R., Ogawa, H.S., Hovestadt, D., Klecker, B., Hilchenbach, M., Möbius, E., Canfield, L.R., Vest, R.E., Watts, R., Tarrio, C., Kühne, M., and Wurz, P., First solar EUV irradiances obtained from SOHO by the CELIAS/SEM, *Sol. Phys.* **177**, 161, 1998.

Judge, D.L., McMullin, D.R., and Ogawa, H.S., Absolute Solar 30.4 nm flux from sounding rocket observations during the solar cycle 23 minimum, *J. Geophys. Res.* **104** A12, 28321–28324, 1999.

McMullin, D.R., Woods, T.N., Dammasch, I.E., Judge, D.L., Lemaire, P., Newmark, J.S., Thompson, W.T., Tobiska, W.K., and Wilhelm, K., Irradiance working group report for the SOHO Inter-Calibration Workshop, this volume, 2002.

McMullin, D.R., Phillips, E., Judge, D.L., Rogers, N., and Ogawa, H.S., Absolute measurements of the solar EUV flux using a rare gas ionization cell, to be submitted, 2002.

McMullin, D.R., Judge, D.L., Phillips, E., Hilchenbach, M., Hovestadt, D., Klecker, B., Ipavich, F., Bochsler, P., Wurz, P., Möbius, E., Galvin, A., and Gliem, F., Helium photoionization rates determined from the CELIAS/SEM instrument on SOHO, to be submitted, 2002.

Newmark, J.S., Cook, J.W., and McMullin, D.R., Solar model EUV and He II irradiances from SOHO EIT derived DEM maps, *Astrophys. J.*, in preparation, 2002.

Ogawa, H.S., Phillips, E., and Judge, D.L., Direct measurements of the helium photoionization rate from sounding rockets, *J. Geophys. Res.* **102**, 11557, 1997.

Samson, J.A.R., He, Z.X., Yin, L., and Haddad, G.N., Precision measurements of the absolute photoionization cross-sections of He, *J. Phys. B* **27**, 887, 1994.

Thompson, W.T., McMullin, D.R., and Newmark, J.S., Comparison of CDS irradiance measurements with SEM and EIT, this volume, 2002.

Torr, M.R., and Torr, D.G., Ionization frequencies for solar cycle 21: Revised, *J. Geophys. Res.* **90**, 6675, 1985.

Torr, M.R., Torr, D.G., Ong, R.A., and Hinteregger, H.E., Ionization frequencies for major thermospheric constituents as a function of solar cycle 21, *Geophys. Res. Lett.* **6**, 771, 1979.

Woods, T., Ogawa, H.S., Tobiska, W.K., and Farnil, F., SOLERS22 WG-4 and WG-5 report, *Sol. Phys.* **177**, 511, 1998.